Influence of mesoporous phosphotungstic acid on the physicochemical properties and performance of sulfonated poly ether ether ketone in proton exchange membrane fuel cell

Mohd Hilmi Mohamed [a,b], Hamid Ilbeygi [c,], Juhana Jaafar [b,**], Madzlan Aziz [a,b], M.H.D. Othman [b], Mukhlis A. Rahman [b]*

[a] *Department of Chemistry, Faculty of Science, Universiti Teknologi Malaysia, 81310, Johor Bahru, Johor, Malaysia*
[b] *N29a, Advanced Membrane Technology Research Centre, School of Chemical and Energy Engineering, Faculty of Engineering, Universiti Teknologi Malaysia, 81310, Johor Bahru, Johor, Malaysia*
[c] *Future Industries Institute (FII), STEM, The University of South Australia, Mawson Lakes, SA, 5095, Australia*

HIGHLIGHTS

- Incorporation of porous HPA in SPEEK membrane used as electrolyte layer in PEMFC.
- Physical and chemical properties are being characterized to get the best membrane.
- The performance analysis concluded the highest performing membrane.

GRAPHICAL ABSTRACT
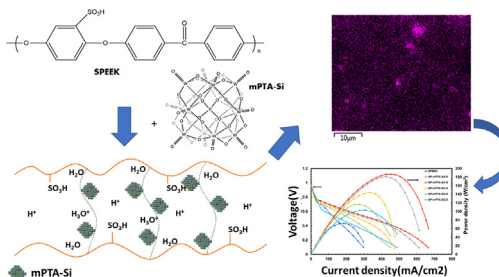
ARTICLE INFO

ABSTRACT

This study demonstrates the successful development of hybrid mesoporous siliceous phosphotungstic acid (mPTA-Si) and sulfonated poly ether ether ketone (SPEEK) as a proton exchange membrane with a high performance in hydrogen proton exchange membrane fuel cells (PEMFC). SPEEK acts as a polymeric membrane matrix and mPTA-Si acts as the mechanical reinforcer and proton conducting enhancer. Interestingly, incorporating mPTA-Si did not affect the morphological aspect of SPEEK as dense membrane upon loading the amount of mPTA-Si up to 2.5 wt%. The water uptake reduced to 14% from 21.5% when mPTA-Si content increases from 0.5 to 2.5 wt% respectively. Meanwhile, the proton conductivity increased to 0.01 Scm^{-1} with 1.0 wt% mPTA-Si and maximum power density of 180.87 mWcm^{-2} which is 200% improvement as compared to pristine SPEEK membrane. The systematic study of hybrid SP-mPTA-Si membrane proved a substantial enhancement

* *Corresponding author.*
** *Corresponding author.*
E-mail addresses: hamid.ilbeygi@unisa.edu.au (H. Ilbeygi), juhana@petroleum.utm.my (J. Jaafar).

Heteropoly acid
Zero emission

in the performance together with further improvement on physicochemical properties of parent SPEEK membrane desirable for the PEMFC application.

Introduction

Soon after Paris agreement in 2016, hydrogen has jumped back on the attention with significant promises for climate change and the global economy. In line with the Sustainable Development Goal (SDG 7) to ensure universal access to affordable, reliable and modern energy services, hydrogen has attained massive attention in recent years as a clean source of future energy. However, the utilization of hydrogen as a fuel has been mitigated due to the lack of efficient fuel cells. In recent years there are several attempts for more efficient hydrogen usage such as in fuel cell and thermophotovoltaic systems [1,2]. As comparison with the other renewable energy systems, the fuel cell known to use hydrogen as the energy source. While alternative sources such as wind and solar cell are the close competitors to the hydrogen fuel cell. However, they still are suffering from various drawbacks as they are highly dependant on climate conditions, for instance, efficient solar cell operation strictly depends on the amount of sun to operate and makes it difficult choice especially country with less sunlight [3]. In addition, wind turbine also faces the similar issues of high dependency on wind power. Considering that, hydrogen fuel cell most suitable choice in terms of continuity of producing electricity and ease of access when its required and also it is independent of the environmental factors. Proton exchange membrane fuel cells (PEMFCs) in particular are great candidates to be used for EVs, portable devices due to their low cost, convenient use and durability. The utilization of hydrogen as feeding fuel in PEMFC can translate the capability of the technology to provide an efficient energy supply at zero emission level. PEMFC converts chemical energy into electrical energy through the oxidation of hydrogen fuel and only produces water vapor as by product [4]. In recent years, the Nafion® membrane has been the main dominator of the electrolyte membrane market and it has been widely studied in PEMFC applications and showed its superior performance and stability for long run [5,6].

Despite the high performance of Nafion® membranes, they still suffer from number of issues such as dehydration and loss of conductivity at elevated temperature [7] due to their low glass transition temperature which also reduces their mechanical strength [8]. Also, they pose high fuel crossover rate which may cause short circuit in PEMFCs and stop their functionality [9]. In addition, the Nafion® high cost is a significant barrier that hinders PEMFC from being widely commercialized [10,11]. Therefore, there have been numerous attempts to mimic the performance of Nafion® from various angles such as developing new polymeric membranes, introducing novel nanomaterials in hybrid membranes etc. [12–14] The vital characteristics for promising materials for PEMFC

electrolyte including i) high proton conductivity at elevated temperature and low relative humidity protons, ii) low fuel crossover, iii) low frequency resistance with electrodes, iv) good stability towards harsh oxidative environment.

Among the various Nafion® alternatives [15], sulfonated poly ether ether ketone (SPEEK) has been proven to be a promising option [12,16,17]. The sulfonation process is a trade-off between the ion conductivity and mechanical properties, which can be controlled by adjusting the hydrophilic and hydrophobic part of the polymer [18]. The polymeric structure of the final membrane can be tailored via engineering the sulfonation process to maximise the proton conduction channels [19]. Beside that, SPEEKs are very economically viable and also demonstrate high mechanical stability and water uptakes at various temperatures [16].

Despite their advantages, the sulfonated polymers also pose few drawbacks. The poor water channels are easily observed due to weak phase separation between hydrophilic and hydrophobic moieties [20]. This also leads to low proton conductivities and excessive swelling behaviour under hydrated conditions. Sulfonated polymer also tends to exhibit lower chemical and oxidative stability as compared to non-sulfonated polymers [21]. In addition, during the sulfonation process it is difficult to reach the balanced sulfonation while the insufficient sulfonation restricts the proton conductivity and the over sulfonation degrades the molecular weight, affecting the water resistance [22].

Introducing SPEEK hybrid membrane can address the aforementioned problems. Addition of proper nanomaterials into SPEEK matrix could provide various advantages to the sulfonated polymer membrane such as enhancing water retention, improving the mechanical stability, increasing the proton conductivity and reducing the fuel cross over [12]. For instance, further addition of clay into sulfonated polysulfone membrane shows good water retention and mechanical strength [23]. Meanwhile the SPEEK doped with zirconium phosphate showed increased conductivity at low humidity and enhanced its chemical stability [24]. Despite the substantial improvement, however, the low power output remains an issue to be solved. Consequently, an inorganic– organic composite electrolytes are attracting increasing interest as one of the key alternative materials development of new proton conductive electrolytes in fuel cell applications [25].

Heteropoly acids (HPAs) are solid acids with high acidity and proton conductivity. They are great candidates for proton exchange membranes with the chemical formula $H_3XM_{12}O_{40}$, where X is a heteropoly atom and M is a transition metal. Phosphotungstic acid ($H_3PW_{12}O_{40}$) (noted as PTA in this work) exhibits the highest acidity and proton conductivity among various types of HPAs [26]. However, they suffer from very low surface area and instability in polar media which limit their

functionality in direct mixing of HPA within the polymeric matrix in PEMFC application [27]. In order to address the aforementioned drawbacks, to date, the main synthesis techniques practiced by researchers were based on incorporating mesoporous silica via nano-casting technique using corrosive acid (HCl), which mitigates process scale-up [28]. Furthermore, the chemical stabilities are also quite unsatisfactory due to their hygroscopicity. However, this can be solved by creating mesopores within the PTA clusters [29]. Recently, Ilbeygi et al. have developed a facile protocol to synthesis siliceous mesoporous PTA (mPTA-Si) via a single soft templating approach. The resultant materials possess desirable properties such as very high surface area, large pore size, high stability in a polar solvent, and uniform spherical morphology [30]. PTA acting as Brønsted acid toward the water molecules of hydration, which is generally weakly bound in the structure, resulting in higher ion conductivity [31].

Considering the excellent properties of SPEEK and mPTA-Si individually as mentioned above, preparing a hybrid membrane can synergistically enhance the final performance for PEMFC application, in this study we introduced various content of mPTA-Si into SPEEK framework for PEMFC application. As per our knowledge there is no report of this hybrid memberane application for PEMFC. As-synthesised SP-mPTA-Si hybrid membranes were further characterized with state of art techniques and undergone PEMFC performance test at 60 and 100% of relative humidity (%RH) operating conditions.

Experimental

Preparation of SPEEK membrane

The SPEEK with the degree of sulfonation of 63 was prepared according to the previous report [12]. The PEEK was obtained from Victrex. Sulphuric Acid (Qrec) and dimethyl sulfoxide (DMSO, Qrec) were used as solvents. 90 wt% percent of DMSO were mixed with 10 wt% of SPEEK to form dope solution. After 3 h of stirring, the mPTA-Si was added to the dope solution followed by continuous stirring for another 24 h. Table 1 shows the composition of the samples.

After all, the polymer and mPTA-Si had been well immersed in the dope solution, about 5 mL of dope solution was poured into 7 cm glass Petri dish. Then, it was dried in a convection oven (UN 110 Memmert, Germany) at 80 °C for 24 h followed by increasing the temperature to 100 °C for 6 h. Finally, the membrane was collected, rinsed and dried at 60 °C.

Table 1 — Composition of SPEEK-mPTA-Si membrane.

Sample	Solvent (wt%)	SPEEK (wt%)	mPTA-Si (wt%)
SPEEK	90	10	0
SP-mPTASi - 0.5			0.5
SP-mPTASi− 1.0			1.0
SP-mPTASi − 1.5			1.5
SP-mPTASi − 2.0			2.0
SP-mPTASi − 2.5			2.5

Characterization of SP-mPTA-Si membrane

Scanning electron microscopy (SEM)
Each membrane was cut into small strips. Then they were immersed in the liquid nitrogen and cut simultaneously. The sample was then placed on the stub and glued with double tape. The process repeated with other samples. Next, it was sputter coated with gold particle for higher resolution images. The imaging has been carried out in a benchtop SEM (Hitachi TM3030) machine at various magnifications. After the images were captured, the images were scanned to obtain the EDX mapping of the samples.

Water uptake
The membrane samples are dried and wiped for excess moisture. Then, all the membrane samples were weighted and recorded as the initial weight. Then, the membrane was immersed in distilled water for 24 h at 80 °C. After that, the membrane was collected, and the excess water was wiped out from the membrane. Finally, the membrane was weighted for their final weight. Eq. (1) shows the calculation of water uptake.

$$Water\ uptake(\%) = \frac{W_O - W_i}{W_i} \times 100 \tag{1}$$

where, Wo is the final weight of membrane after immersed, Wi is the initial weight of membrane prior of immersed. The procedure was repeated for each membrane.

Fourier transform infra-red
The FTIR spectra was done to observe the chemical properties in the mPTA-Si and all membrane samples (pristine SPEEK and SPEEK with mPTA-Si). The spectra were recorded by using Nicolet iS 10 spectrometer (Thermo Scientific) and ATR technique, the sample was put in the scanner and sealed tight before undergone scanning. The scanning rate was set at 32 and the wavenumber from 4000 to 600 cm^{-1}. The process repeated for other samples.

Swelling properties
The membranes were cut in squares of 1 cm^2. Then, the thickness of each sample was measured via calliper. Next, each sample was immersed in distilled water at 80 °C for 24 h. Then, the thickness of sample was remeasured. The swelling was calculated using Eq. (2). The process repeated for other samples.

$$Swelling(\%) = \frac{T_a - T_i}{T_i} \times 100 \tag{2}$$

where T_a is the weight of the sample after the immersion while T_i is the initial weight of the sample.

Proton conductivity
Each membrane was cut into 1.5 cm in diameter. Then, it was immersed in distilled water at room temperature for 24 h. After that, the membrane proton conductivity was measured via 2 probe sample holders, connected to autolab (PGSTAT302 N). After that, the resistance was recorded, and the conductivity was calculated via Eq. (3).

$$C = \frac{R \times T_m}{A} \qquad (3)$$

where C is the conductivity in Scm^{-1}, R is the resistance of the membrane, T_m is the thickness of the membrane and A is the area of the membrane.

Hydrogen permeation

The membrane was cut in circles with diameter of 5.5 cm. Then, the membrane was put into the cell test. The membrane was enclosed and tightly screwed to prevent outside gas entered the cell. Next, the hydrogen gas was flown to the membrane surface starting from 2 bar and gradually increased to 16 bar. The volume for hydrogen to move recorded and calculated by Eq. (4).

$$Hydrogen\ permeation = \frac{V \times L}{A \times t \times \Delta P} \qquad (4)$$

where V is the volume of gas permeated, L is the thickness of the membrane, A is the area of the sample, t represents the time required to permeate the gas and ΔP is the partial pressure applied into the membrane. The process repeated for other samples.

Mechanical testing

The mechanical strength was done by using Instron (4240, ASTM D882) with speed of 10 mm/min The sample was cut into 1 cm in width prior to the test. The sample then clamped at top and bottom. The device then pulled both top and bottom of the sample until it reached 80% stress threshold. Finally, the value of the tensile strength recorded. For each sample, 5 repetitions have been done and average value has been reported.

PEMFC performance testing

The membrane samples were cut into 3 cm × 3 cm in square. Meanwhile, the Pt (Fuel Cell Earth) electrodes were cut into 1.5 × 1.5 cm. Then the membrane was sandwiched between the electrode and undergone hot press at 5 bar and 60 °C for 1 min. Then the complete sample was put into testing system (850e Fuel Cell Test System Scribner Associates, USA). The fuel and oxidant were both set at 600 cc min^{-1}. The humidity was set at 60 and 100% and the working temperature was maintained at 80 °C.

Results and discussion

Characterization of SP-mPTA-Si membrane

Confirmation of chemical bonding

Fig. 1 shows the FTIR of pristine SPEEK, mPTA–Si powder and SP-mPTA-Si membrane ranging from 4000 to 600 cm^{-1}. For All the membranes the peak at around 3450 cm^{-1} indicating the presence of –OH, bands at 1286 and 1080 cm^{-1} which are referring to asymmetrical and symmetrical stretching vibrations of O=S=O group respectively were observed. There are
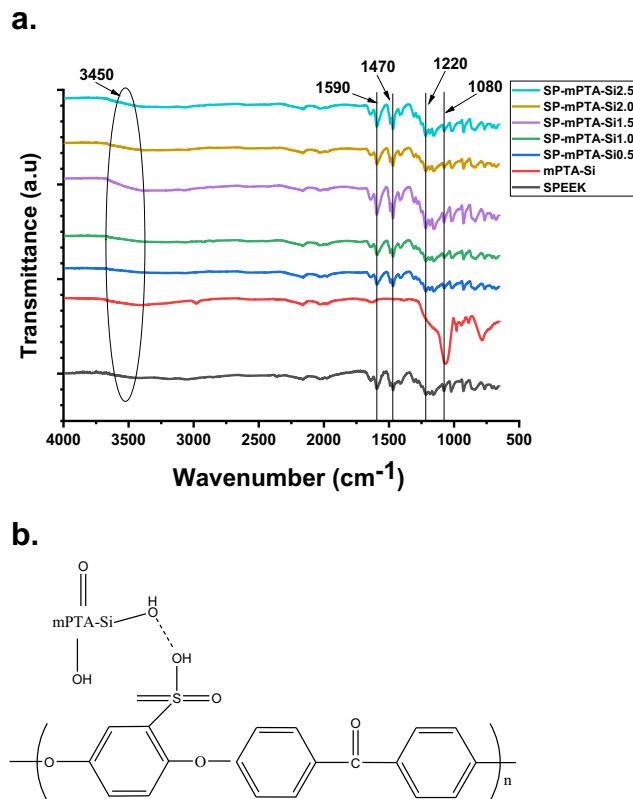
Fig. 1 – a) FTIR spectra of SPEEK, solid mPTA-Si and SP-mPTA-Si membrane at different mPTA-Si loading. b) interaction of mPTA-Si with SPEEK membrane.

also stretching vibrations of C = C in the aromatic ring at 1590 and 1470 cm^{-1} [32].

Meanwhile, mPTA-Si signal at around 1080, 983, 1900 and 800 cm^{-1} indicating the presence of P–O, W-O_t, W-O_c-W and W-O_e-W stretching vibrations. Where O_t, O_c and O_e are referring to terminal, corner and edge oxygen [33]. There is a strong and broad band at 3400 cm^{-1} which corresponds to the O–H stretching vibrations of the hydroxyl group in the mPTA-Si. After the addition of mPTA-Si on the SPEEK membrane, the presence of mPTA-Si characteristic did not affect the SPEEK FTIR signal which indicating the membrane characteristic remains unchanged. This shows that the mPTA-Si doesn't interfere with the chemical structure of the SPEEK. The peaks for SPEEK remains unchanged with the increased amount of mPTA-Si. However, there are slight changes peak intensity at 1080 cm^{-1} indicating the P–O content increasing which translate into the higher amount of mPTA-Si content in the membrane. In the schematic of interaction between mPTA-Si and SPEEK, the primary structure of mPTA-Si, protons interact with the bridging oxygen because the basicity of the bridging oxygen and not with the terminal oxygen. Meanwhile, in the hydrated form of mPTA-Si, it was established in the previous study that the terminal oxygen atoms of the anions associate with the $H_5O_2^+$ bridges to generate secondary structure [34]. The results clearly indicating the sulfonic group are not affected by introducing the mPTA-Si into SPEEK. Therefore, a fundamental characteristic of SPEEK still intact.
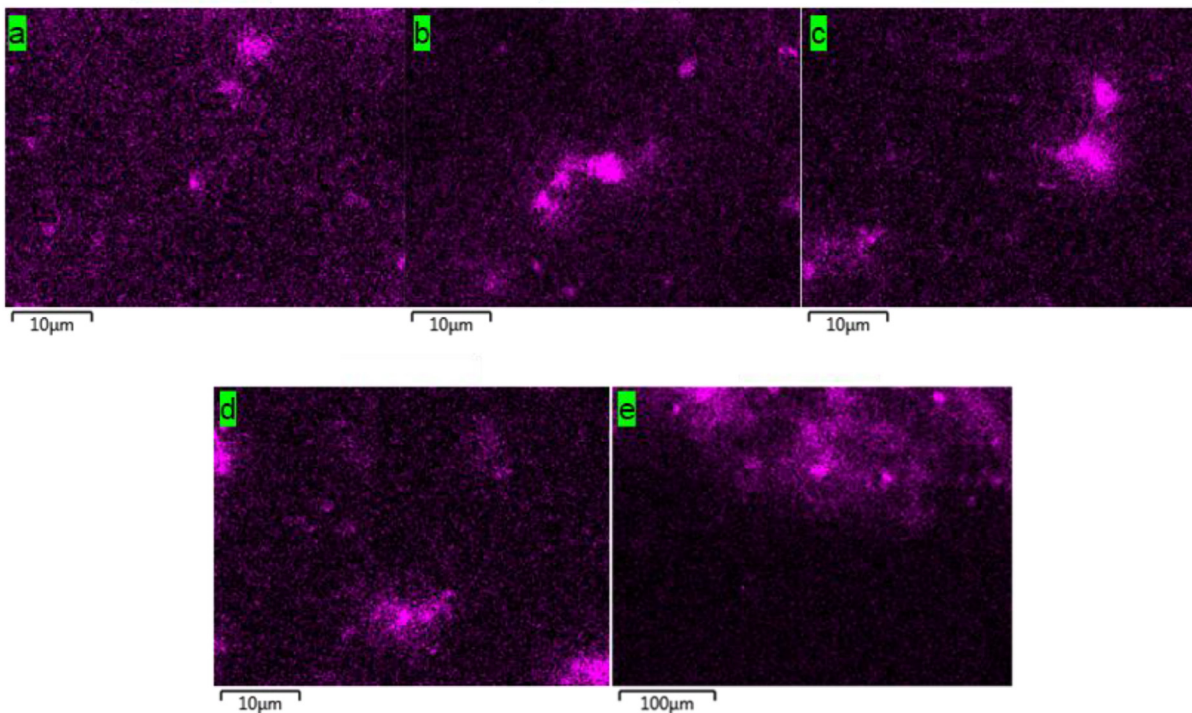
i)
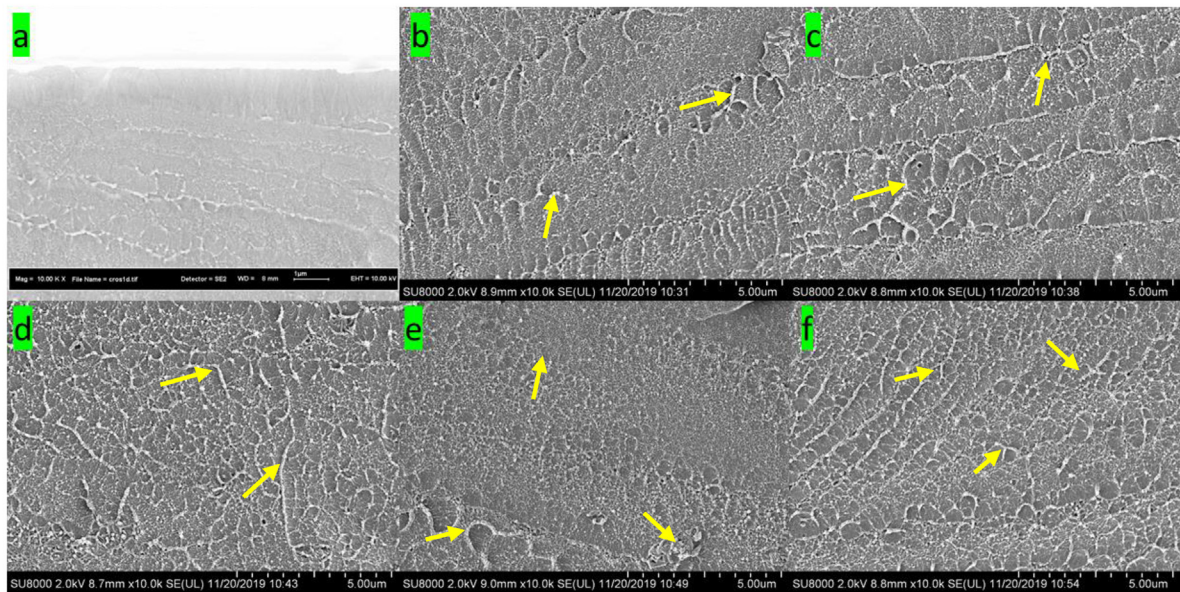
ii)

Fig. 2 — (i) SEM images of a)SPEEK b)SP-mPTA-Si0.5 c)SP-mPTA-Si1.0 d)SP-mPTA-Si1.5 e)SP-mPTA-Si2.0 f)SP-mPTA-Si2.5 membrane. The yellow arrow indicating the globular like structure on the membrane cross section. (ii) The EDX images of the samples. (The black area represent the SPEEK meanwhile the purple area corresponding to W component in mPTA-Si) a) SP-mPTA-Si0.5 b) SP-mPTA-Si1.0 c) SP-mPTA-Si1.5 d) SP-mPTA-Si2.0 e) SP-mPTA-Si2.5. (For interpretation of the references to color in this figure legend, the reader is referred to the Web version of this article.)

Morphology of the hybrid SP-mPTA-Si membranes

Fig. 2 shows the cross-section morphology of the membrane. The thickness of the membrane was observed to be around 80 μm which is within the intrinsic thickness of a membrane should have as an electrolyte. As expected, all membranes have a dense symmetric structure which can limit the H_2 fuel crossover across the membrane and is an ideal feature for PEMFC application.

After the addition of 0.5 wt% of mPTA-Si, it was observed the spherical like shape was scattered surrounding the cross section of membrane. Increasing the mPTA-Si content to 1.0%, leads to connection of the spherical or globular like structure to each other creating a wormlike morphology. This indicates that the addition of the mPTA-Si does changes the morphology in terms of having larger surface area; thus, provides more spaces for proton hopping to occur. Meanwhile, the EDX mapping shows the distribution of mPTA-Si across the membrane. It can be observed the mPTA-Si widely dispersed at 0.5 until 1.5. However, it can be seen there are agglomeration occurred. This due to the mPTA-Si have reached the threshold for SPEEK membrane. It also indicating the SPEEK membrane physical properties undergone significant changes in terms of dense properties. Such agglomeration reduces the dense properties of the membrane thus the changes can be observed in hydrogen permeability. Less dense will allow more hydrogen to pass through across the membrane.

Water uptake analysis and proton conductivity

Water uptake analysis was carried out to measure the ability of the membrane to absorb water. Fig. 3 shows the water uptake and proton conductivity of parent SPEEK and mPTA-Si incorporated SPEEK membranes. The water uptake of the membrane recorded about 21.5% for 0.5 wt% of mPTA-Si content. When the content of mPTA-Si increased to 1.0%, there is a slight decrease at 21% of water uptake. Then, the water uptake recorded had slight increase to 20%, 17% and 14% when the content of mPTA-Si increased to 1.5, 2.0 and 2.5 wt% respectively. From this observation, it was clear that the mPTA-Si
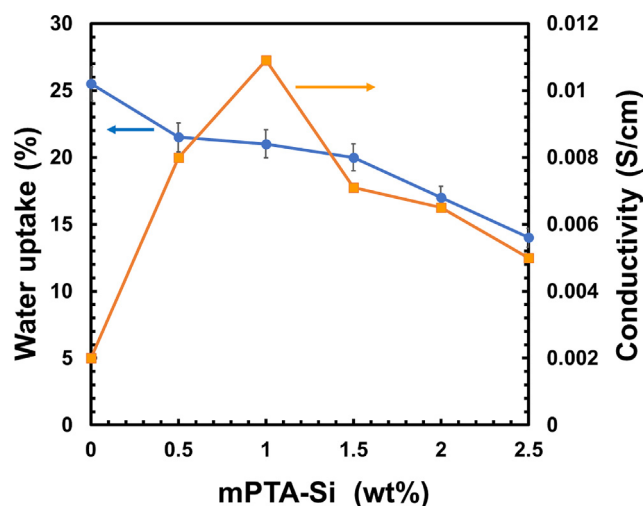
content does reduce the water uptake properties of the membrane. It was due to the mPTA-Si properties that already holds up a significant amount of water content [35]. When it reached the threshold, there are less water uptake recorded.

The proton conductivity measurement was done to determine the ability of the sample conducting the proton across the membrane. Fig. 4 shows the proton conductivity of the sample containing different amount of mPTA-Si loading. The proton conductivity was recorded at 0.008 Scm^{-1} and increased to 0.011 Scm^{-1} when the mPTA-Si content increased from 0.5 to 1.0 wt%, respectively. Beyond 1.0 wt% of mPTA-Si loading, the proton conductivity decreased as mPTA-Si loading increased and recorded as low as 0.005 Scm^{-1}. In comparison, the pristine SPEEK conductivity was recorded at 0.002 Scm^{-1}. It does show the additional of mPTA-Si causes slight improvement in the proton conductivity courtesy of the mPTA-Si acidic properties that enables water diffusion and proton transport via hopping mechanism. Initially, the trends increase up to 1.5 wt% of addition causing the conductivity to be declined. This could be due to the decreasing of the dense properties of the membrane caused by separation of polymer chains. The globular like morphology increasing as shown in the SEM images contributed into less dense membrane structure which reduces the number of protons hopping across the membrane.

Transport mechanism

Thermodynamic understanding of the proton conduction in SPEEK membrane involves the activation energy of proton transport across the cell. The temperature dependence of proton conductivity can be described into Arrhenius equation. The trends for temperature dependent proton conductivity of the membranes can be seen in Fig. 4, where the slopes represent the activation energy that can be derived by using Eq. (5):

$$\ln \sigma = \ln A - \frac{E_a}{RT} \tag{5}$$

where A is the pre-exponential factor, R is the ideal gas constant (8.314 J K^{-1} mol^{-1}) and T is temperature (K). The fitting of

Fig. 3 — Water uptake analysis and proton conductivity of the SP-mPTA-Si membrane.
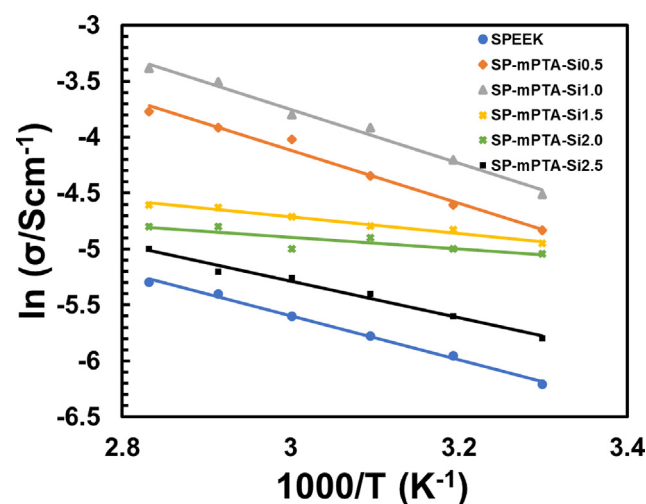

Fig. 4 — Arrhenius plot for the proton conductivity as a function of temperature at different mPTA-Si content.

the slope represents the activation energy for each sample. Initially, the SPEEK recorded activation energy of 36 kJ/mol indicating the dominant mechanism is Grotthus mechanism (E_a range between 14.0 and 40.0 kJ/mol) [36]. Meanwhile, the E_a recorded at 37—40 kJ/mol after addition of mPTA-Si showing the E_a increased with the adding more amount of mPTA-Si. A slight increase in activation energy after mPTA-Si is added can be due to decreasing of the water uptake. Furthermore, less water content in the membrane means there are fewer proton conducting pathways to transfer proton as demonstrated from the water uptake data where the excess mPTA-Si causing the membrane to absorb less water [37].

Hydrogen permeability

The hydrogen permeability measures the ability of the membrane to allow gas being transport across the membrane. The correlation between the hydrogen pressure and flux are present in Fig. 5. Membrane that could withstand high pressure will prevent gas transport and only allow proton to cross the membrane. For each sample, the pressure was being manipulated from 2 bar to 16 bar. Beyond 16 bar, there permeability is very quick indicating the membrane samples are being cracked courtesy by the heavy pressure of the hydrogen gas. In Fig. 8, it can be seen the slope increases as the amount of the mPTA increases. It also can be seen the permeability is directly proportional to the differential pressure between feed and permeate sides of the membrane. Initially, the slope value was 2×10^{-13} mol $m^2s^{-1}bar^{-1}$ at pristine SPEEK. Then, it increases up to 2.00×10^{-12} $m^2s^{-1}bar^{-1}$ at SP-mPTA-Si 2.0.

There are similar values of permeation across all samples recorded at 2 bar of hydrogen pressure indicating there is less hydrogen pass through the membrane due to lack of pressure driven. After increasing the hydrogen pressure, a different gradient slope shows the pressure does drive more hydrogen to pass through the membrane [38]. It can clearly be seen the presence of microchannels does lessen the dense properties of the membrane resulting in more hydrogen able to permeate. Reduction of the membrane dense clearly can be
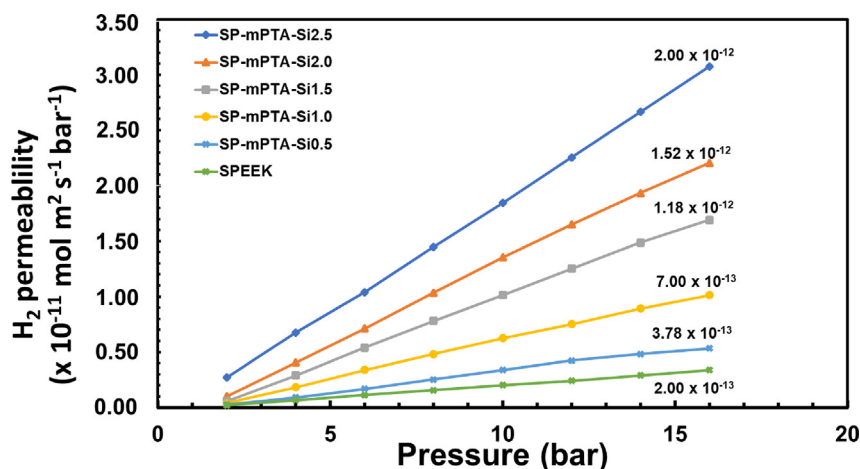

Fig. 6 — Mechanical properties of the membranes at different mPTA-Si content.

observed at higher hydrogen pressure. At 16 bar, the pristine SPEEK recorded at 3.38×10^{-12} $m^2s^{-1}bar^{-1}$ and the permeability increases until SP-mPTA-Si 2.5 recorded 3.08×10^{-11} $m^2s^{-1}bar^{-1}$. This because of the mPTA-Si had created porous microstructure which facilitates hydrogen permeation with less hydrogen permeation resistance. It can be observed from the EDX mapping the agglomeration produces a less dense membrane thus allowing more hydrogen to pass through.

On the other hand, the selectivity of the membrane depends on the addition of mPTA-Si. The selectivity measures the membrane to produce electricity and minimise the production of undesirable side products [39]. Table 2 summarize the selectivity of the all the sample in this study. The selectivity was calculated by dividing the conductivity and permeability data by using Eq. (6).

$$Selectivity = \frac{C}{P} \qquad (6)$$

Fig. 5 — Hydrogen permeability of the membranes at different mPTA-Si content and at different gas pressure. (The number displayed at pressure 16 bar is the gradient slope for each sample).
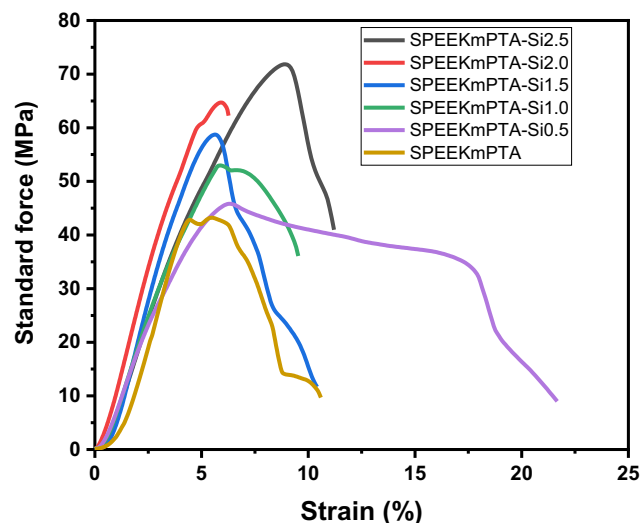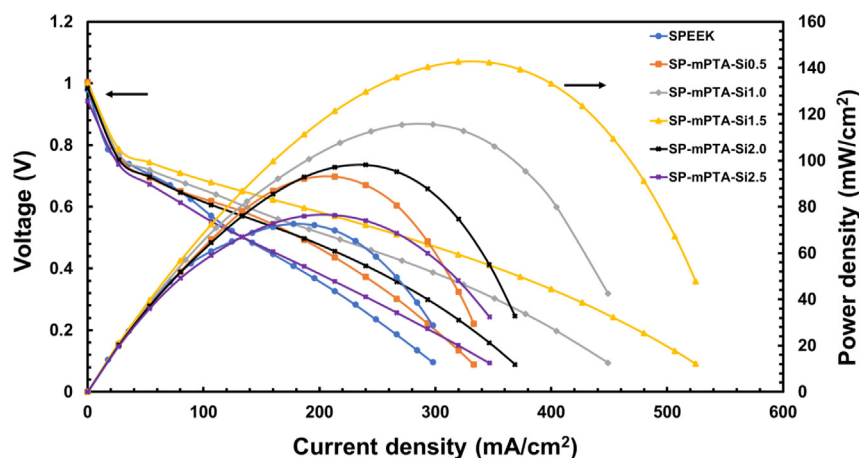
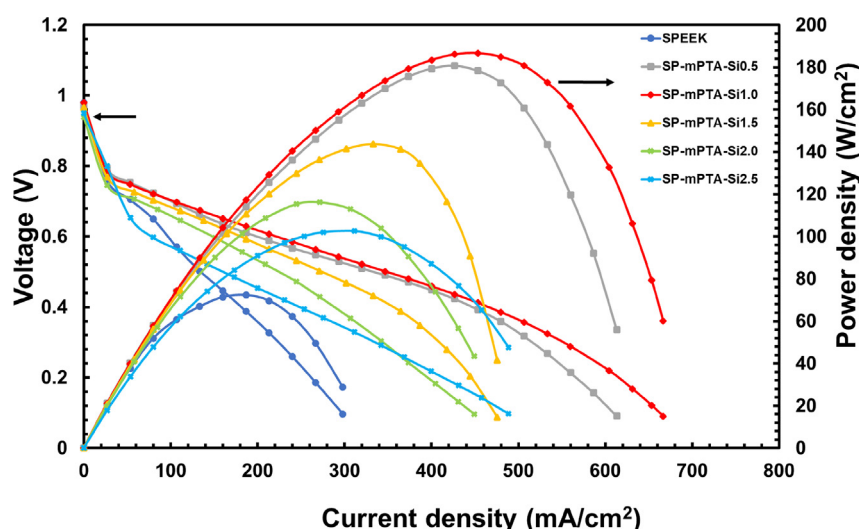**Fig. 7** – Performance test of SPEEK membrane with different mPTA-Si content at 60% RH.

Fig. 8 – Performance test of SPEEK membrane at different mPTA-Si content at 100% RH.

Table 2 – Comparison between SPEEK membrane and all the composite in this study.

Sample	Proton conductivity (S/cm)	H_2 permeability[a] ($\times 10^{-11}$ m^{2}s^{-1}bar^{-1})	Selectivity (mol.S.s.bar/cm^3)	Maximum power density (mWcm^{-2})	
				RH60	RH100
SPEEK	0.002	20.00	10,000	72.59	72.42
SP-mPTA-Si 0.5	0.008	37.80	2116.40	93.07	180.72
SP-mPTA-Si 1.0	0.0109	70.00	1557.14	115.51	186.73
SP-mPTA-Si 1.5	0.0071	1.18	601.70	142.65	143.71
SP-mPTA-Si 2.0	0.0065	1.52	4276.32	98.12	116.29
SP-mPTA-Si 2.5	0.005	2.00	2500	76.35	102.56

[a] Value for H_2 permeability were taken at pressure 2 bar, which replicate the flowrate of the fuel during performance test.

where C is the conductivity and P is the permeability of the membrane. It was observed the SPEEK had highest selectivity recorded at 10,000 S s bar/cm^3 due to its good proton conductivity and hydrogen permeability. After the amount of mPTA-Si increases, the selectivity decreases as well. The lowest recorded at 601.695 S s bar/cm^3 at 1.5 mPTA-Si. The main factor contributed in decreasing in selectivity can be the increased spacing of the polymer in the membrane due to mPTA-Si presence causing the distance of the sulfone group increases from each other; causing the decrease in performance [40]. However, the silica content in the mPTA-Si could benefit electrochemical performance and increase the mobility of proton [41]. After a certain extent of loading, the selectivity increases due to the proton transport path will become

tortuous as referred to the SEM images where the agglomeration can be observed as the amount of mPTA-Si increases.

Mechanical strength

The mechanical testing was done to measure the ability of the membrane to stand force until it reaches a threshold. Fig. 6 shows the mechanical strength for all samples involved. It was observed the pristine SPEEK recorded the lowest mechanical strength at 43.46 MPa. After the addition of mPTASi, the mechanical strength increased to 64.66 MPa at 0.5 mPTASi and the trend continues till the highest recorded at 71.8 MPa when the mPTA-Si content increased to 2.5. The elongation break for samples is between 5 and 10% indicating the mPTA-Si did not change the membrane moduli properties. The increase in mechanical properties can be related to the interactions between mPTA-Si and the sulfonated polymer, creating a reinforcement mechanism. In such case of additional of clay into the membrane, it was proved that the membrane mechanical strength increases to 10% from the prior addition [42]. Furthermore, the increase of mechanical strength also indicating the mPTA-Si promotes interaction of SO_3H groups within the SPEEK layer [43].

Performance testing

The performance evaluation was carried out to determine the membrane ability as an electrolyte for PEMFC. Figs. 7 and 8 shows the performance of the membrane. The condition of the testing was set at constant temperature of 80 °C and 60% and 100% relative humidity (RH). The OCV for most of the samples recorded at around 1.0 V indicating there are no significant crossover of the proton courtesy of the dense structure of the membrane. In addition, low ohmic polarization can be predicted, due to the high OCV. Fig. 7 shows the power density of SPEEK with the addition of mPTA-Si.

It can be observed the pristine SPEEK membrane shows the power density of 72.42 mWcm^{-2}. When the mPTA-Si introduced into the SPEEK, the power density increases to 93.07 mWcm^{-2} for 0.5 wt%. Then, the power density increases to 115.5 mWcm^{-2} after the addition of mPTA-Si increases to 1.0 wt%. Afterwards, the increase of power density to 142.65 mWcm^{-2} after the addition of 1.5 wt%. However, it can be seen the power density decreases to 98.12 and 76.35 mWcm^{-2} when the amount of mPTA-Si increases to 2.0 and 2.5 wt% respectively. The reduction of power density mostly contributed by increasing of the fuel crossover as shown in the hydrogen permeability data. It also indicates there is a threshold on how much the mPTA-Si requires until power density drops. Furthermore, it shows that the progressive effect on PEMFC performance is caused by the mPTA-Si towards membrane. Acidic properties mPTA-Si causes the membrane to have higher amount of water groups via their sulfonic acid groups and hygroscopic properties of mPTA-Si.

From Fig. 8, the cell performance increased until the mPTA-Si content 1.5 wt%. This indicates that the improvement induced by the mPTA-Si become more pronounced as the mPTA-Si content increases. However, reduction in power density can be due to the interface of the mPTA-Si with the proton transport pathway; subsequently, the lower number of protons involved in the reaction [44]. Interestingly, at RH of 100% that effect been eliminated. Fig. 8 shows the performance at RH 100%.

Initially, the SPEEK membrane without additive was recorded at 72.42 mWcm^{-2}. When the SP-mPTA-Si 0.5 membrane displays the power density of 180.87 mWcm^{-2}. Then, the power density increases to 187.00 Wcm^{-2} after the addition of mPTA-Si increases to 1.0 wt%. It was observed there is a huge leap after the addition at only 1 wt% of mPTA-Si. However, it can be seen the power density decreases to 143.78, 116.13 and 102.56 mWcm^{-2} when the amount of mPTA-Si increases to 1.5, 2.0 and 2.5 wt% respectively. It can be observed the mPTA-Si increase the power density due to the increases of water retention via hygroscopic properties of mPTA-Si. However, the decrease in power density can be related to the agglomeration of mPTA-Si that can be observed in the SEM morphology and conductivity. The agglomeration leads to the decrease of dense properties of the membrane [45]. Consequently, the further increase of mPTA-Si also decreases the conductivity which leads to a decrease in the power density.

When RH increased to 100%, there was a contradiction found as compared to RH 60%. The mPTA-Si with 1.0 wt% recorded the highest power density at RH 100% while at RH 60% the 1.5 wt% recorded the highest power density. The power density at low humidity can be related to the high ionic resistance of the mPTA-Si. As humidity increases, the active zone will expand to decrease the activation overpotential. In addition, the pores in the membrane would be more flooded due to the lower water removal rate and the concentration overpotential would be larger in higher humidity [46]. On top of that, the low RH can depress the electrode kinetics, including electrode reaction and mass diffusion rates, and proton conductivity as well resulting in a degradation in fuel cell performance [47]. Table 3 shows the effect of the RH towards performance of the fuel cell based on the report from previous study. The resulting power density from this study is comparable from the previous performance. From the table, it can be concluded that PEMFC does relies on the RH to achieve good performance. However, the resulting power output also comes from the membrane electrode assembly (MEA) material and properties that able to cope with certain condition.

Table 3 – Comparison of power density when differ RH is applied.

Materials	RH	Temperature (°C)	Power density (W/cm²)	Voltage (V)	References
Nafion - ionomer	60	60	0.14	0.96	[46]
Nafion	100	120	0.50	0.90	[47]
Aerogel	75	70	0.10	0.40	[48]
SPEEK/PBI	60	80	0.11	0.0.85	[49]
SPEEK-mPTA-Si	100	80	0.16	0.81	This work

Conclusion

In this study, we have successfully fabricated SP-mPTA-Si hybrid membranes with various SP content. The SEM images show there are no significant changes except the increases of spherical shape were observed. The EDX mapping demonstrats the mPTA-Si widely spread across the membrane. While, the water uptake decreases with the increased amount of mPTA-Si, the conductivity increases at 1.0 wt% of mPTA-Si and decrease after more mPTA-Si added. The hydrogen permeability recorded highest at 2.5 wt% of mPTA − Si indicating excessive fillers will increases the porosity of the membrane. Meanwhile the mechanical strength shows the highest recorded when 2.5 wt% of mPTA-Si added shows the filler able to decrease the polymer boundaries. The OCV was recorded at 1.0 V for all of samples which indicates the membranes are dense structure. The maximum power density for SPEEK initially recorded at 72.42 mWcm^{-2} and the best performance was when 1.0 wt% of mPTA-Si added where the maximum power density increases to by over 200% to 187.00 mWcm^{-2} at RH 100%. Thus, the SP-mPTA-Si 1.0 demonstrate a very promising performance to be employed as an efficient electrolyte membrane for medium temperature PEMFC application. Furthermore, the mPTA-Si did not interfere the mechanical properties makes it suitable to be applied as filler due to the SPEEK is well known having good mechanical properties.

Declaration of competing interest

The authors declare that they have no known competing financial interests or personal relationships that could have appeared to influence the work reported in this paper.

Acknowledgement

REFERENCES

[1] Zuo W, Li J, Zhang Y, Li Q, He Z. Effects of multi-factors on comprehensive performance of a hydrogen-fueled micro-cylindrical combustor by combining grey relational analysis and analysis of variance. Energy 2020;199:117439.

[2] Zuo W, Zhang Y, Li Q, Li J, He Z. Numerical investigations on hydrogen-fueled micro-cylindrical combustors with cavity for micro-thermophotovoltaic applications. Energy 2021;223:120098.

[3] Cheng S, Zhao G, Gao M, Shi Y, Huang M, Marefati M. A new hybrid solar photovoltaic/phosphoric acid fuel cell and energy storage system; Energy and Exergy performance. Int J Hydrogen Energy 2021;46:8048—66.

[4] B. Sørensen, G. Spazzafumo, 3 - fuel cells, in: B. Sørensen, G. Spazzafumo (Eds.) Hydrogen and fuel cells (3rd ed.), Academic Press2018, pp. 107-220.

[5] Kim J, Jeon J-D, Kwak S-Y. Nafion-based composite membrane with a permselective layered silicate layer for vanadium redox flow battery. Electrochem Commun 2014;38:68—70.

[6] Hou HY, Polini R, Di Vona ML, Liu XX, Sgreccia E, Chailan JF, Knauth P. Thermal crosslinked and nanodiamond reinforced SPEEK composite membrane for PEMFC. Int J Hydrogen Energy 2013;38:3346—51.

[7] Garsany Y, Gould BD, Baturina OA, Swider-Lyons KE. Comparison of the sulfur poisoning of PBI and nafion PEMFC cathodes. Electrochem Solid St 2009;12:B138—40.

[8] Bose AB, Zhu X. Design of stable and durable polymer electrolyte membrane fuel cells by embedding hydrophobic cage-structured material in cell components. Fuel 2019;235:954—61.

[9] Malers JL, Sweikart MA, Horan JL, Turner JA, Herring AM. Studies of heteropoly acid/polyvinylidenedifluoride-hexafluoroproylene composite membranes and implication for the use of heteropoly acids as the proton conducting component in a fuel cell membrane. J Power Sources 2007;172:83—8.

[10] Branco CM, El-kharouf A, Du S. Materials for polymer electrolyte membrane fuel cells (PEMFCs): electrolyte membrane, gas diffusion layers and bipolar Plates☆. In: Olabi A-G, editor. Encyclopedia of smart materials. Oxford: Elsevier; 2022. p. 378—88.

[11] Zuo W, Li J, Zhang Y, Li Q, Jia S, He Z. Multi-factor impact mechanism on combustion efficiency of a hydrogen-fueled micro-cylindrical combustor. Int J Hydrogen Energy 2020;45:2319—30.

[12] Jaafar J, Ismail AF, Matsuura T, Nagai K. Performance of SPEEK based polymer—nanoclay inorganic membrane for DMFC. J Membr Sci 2011;382:202—11.

[13] Nagarale RK, Heller A, Shin W. A stable Ag/ceramic-membrane/Ag2O electroosmotic pump built with a mesoporous phosphosilicate-on-silica frit membrane. J Electrochem Soc 2012;159:P14—7.

[14] Nouel KM, Fedkiw PS. Nafion®-based composite polymer electrolyte membranes. Electrochim Acta 1998;43:2381—7.

[15] Ilbeygi H, Mayahi A, Ismail AF, Nasef MM, Jaafar J, Ghasemi M, Matsuura T, Zaidi SMJ. Transport properties of SPEEK nanocomposite proton conducting membranes: optimization of additives content by response surface methodology. J Taiwan Inst Chem Eng 2014;45:2265—79.

[16] Ilbeygi H, Ismail AF, Mayahi A, Nasef MM, Jaafar J, Jalalvandi E. Transport properties and direct methanol fuel cell performance of sulfonated poly (ether ether ketone)/Cloisite/triaminopyrimidine nanocomposite polymer electrolyte membrane at moderate temperature. Separ Purif Technol 2013;118:567—75.

[17] Mayahi A, Ilbeygi H, Ismail AF, Jaafar J, Daud WRW, Emadzadeh D, Shamsaei E, Martin D, Rahbari-Sisakht M, Ghasemi M, Zaidi J. SPEEK/cSMM membrane for simultaneous electricity generation and wastewater treatment in microbial fuel cell. J Chem Technol Biotechnol 2015;90:641—7.

[18] Kim AR, Park CJ, Vinothkannan M, Yoo DJ. Sulfonated poly ether sulfone/heteropoly acid composite membranes as electrolytes for the improved power generation of proton exchange membrane fuel cells. Compos B Eng 2018;155:272—81.

[19] Muthumeenal A, John Rethinam A, Nagendran A. Sulfonated polyethersulfone based composite membranes containing heteropolyacids laminated with polypyrrole for electrochemical energy conversion devices. Solid State Ionics 2016;296:106−13.

[20] Dong X, Hou S, Mao H, Zheng J, Zhang S. Novel hydrophilic-hydrophobic block copolymer based on cardo poly(arylene ether sulfone)s with bis-quaternary ammonium moieties for anion exchange membranes. J Membr Sci 2016;518:31−9.

[21] Wang J, Zhao C, Zhang L, Li M, Ni J, Wang S, Ma W, Liu Z, Na H. Cross-linked proton exchange membranes for direct methanol fuel cells: effects of the cross-linker structure on the performances. Int J Hydrogen Energy 2012;37:12586−96.

[22] Unveren EE, Erdogan T, Çelebi SS, Inan TY. Role of post-sulfonation of poly(ether ether sulfone) in proton conductivity and chemical stability of its proton exchange membranes for fuel cell. Int J Hydrogen Energy 2010;35:3736−44.

[23] Ilbeygi H, Ghasemi M, Emadzadeh D, Ismail AF, Zaidi SMJ, Aljlil SA, Jaafar J, Martin D, Keshani S. Power generation and wastewater treatment using a novel SPEEK nanocomposite membrane in a dual chamber microbial fuel cell. Int J Hydrogen Energy 2015;40:477−87.

[24] Lakshminarayana G, Nogami M. Synthesis and characterization of proton conducting inorganic−organic hybrid nanocomposite membranes based on tetraethoxysilane/trimethylphosphate/3-glycidoxypropyltrimethoxysilane/heteropoly acids. Electrochim Acta 2009;54:4731−40.

[25] Oh SY, Yoshida T, Kawamura G, Muto H, Sakai M, Matsuda A. Proton conductivity and fuel cell property of composite electrolyte consisting of Cs-substituted heteropoly acids and sulfonated poly(ether-ether ketone). J Power Sources 2010;195:5822−8.

[26] Ilbeygi H, Kim IY, Kim MG, Cha W, Kumar PSM, Park D-H, Vinu A. Highly crystalline mesoporous phosphotungstic acid: a high-performance electrode material for energy-storage applications. Angew Chem Int Ed 2019;58:10849−54.

[27] Zaidi SMJ, Mikhailenko SD, Robertson GP, Guiver MD, Kaliaguine S. Proton conducting composite membranes from polyether ether ketone and heteropolyacids for fuel cell applications. J Membr Sci 2000;173:17−34.

[28] Janik MJ, Bardin BB, Davis RJ, Neurock M. A quantum chemical study of the decomposition of keggin-structured heteropolyacids. J Phys Chem B 2006;110:4170−8.

[29] Pugazhenthiran N, Ramkumar S, Sathish Kumar P, Anandan S. In-situ preparation of heteropolytungstic acid on TiMCM-41 nanoporous framework for photocatalytic degradation of textile dye methyl orange. Microporous Mesoporous Mater 2010;131:170−6.

[30] Ilbeygi H, Sawant DP, Ruban SM, Reshma KS, Umbarkar SB, Halligudi SB, et al. Direct synthesis of mesoporous siliceous phosphotungstic acid and its superior catalytic activity on the cyclohexylation of phenol. J Phys Chem C 2021;125(12):6723−34.

[31] Kreuer K-D. Proton conductivity:materials and applications. Chem Mater 1996;8:610−41.

[32] Wan Mohd Noral Azman WNE, Jaafar J, Salleh WNW, Ismail AF, Othman MHD, Rahman MA, Rasdi FRM. Highly selective SPEEK/ENR blended polymer electrolyte membranes for direct methanol fuel cell. Mater Today Energy 2020;17:100427.

[33] Rao U, Sekharnath KV, S H, Rao KC, Subha MCS. Mixed matrix membranes of sodium alginate and hydroxy propyl cellulose loaded with phosphotungstic heteropolyacid for the pervaporation separation of water-isopropanol mixtures at 30 °c. Int J Scientific & Technol Res 2014;3:129−37.

[34] Kumari M, Sodaye HS, Bindal RC. Effect of phosphotungstic acid blending on properties of sulfonated poly(ether ether ketone)−poly(ethylene glycol) crosslinked membranes. J Appl Polym Sci 2018;135:46667.

[35] Heravi MM, Vazin Fard M, Faghihi Z. Heteropoly acids-catalyzed organic reactions in water: doubly green reactions. Green Chem Lett Rev 2013;6:282−300.

[36] Zhai S, Dai W, Lin J, He S, Zhang B, Chen L. Enhanced proton conductivity in sulfonated poly(ether ether ketone) membranes by incorporating sodium dodecyl benzene sulfonate. Polymers 2019;11:203.

[37] Li L, Xu L, Wang Y. Novel proton conducting composite membranes for direct methanol fuel cell. Mater Lett 2003;57:1406−10.

[38] Patil MB. Synthesis and characterization of heteropolyacid (H3PW12O40) embedded poly (vinyl alcohol)-g-acrylamide copolymeric membranes and their evaluation for proton exchange membrane fuel cells. Mater Sci for Energy Technol 2020;3:846−52.

[39] Chia MY, Thiam HS, Leong LK, Koo CH, Saw LH. Study on improvement of the selectivity of proton exchange membrane via incorporation of silicotungstic acid-doped silica into SPEEK. Int J Hydrogen Energy 2020;45:22315−23.

[40] Mulcherjee R, Mandal AK, Banerjee S. Sulfonated poly(arylene ether sulfone) functionalized polysilsesquioxane hybrid membranes with enhanced proton conductivity. E-Polymers 2020;20:430−42.

[41] Ren JN, Zhang SL, Liu Y, Wang Y, Pang JH, Wang QH, Wang GB. A novel crosslinking organic-inorganic hybrid proton exchange membrane based on sulfonated poly(arylene ether sulfone) with 4-amino-phenyl pendant group for fuel cell application. J Membr Sci 2013;434:161−70.

[42] Simari C, Enotiadis A, Nicotera I. Transport properties and mechanical features of sulfonated polyether ether ketone/organosilica layered materials nanocomposite membranes for fuel cell applications. Membranes 2020;10:87.

[43] Lee K-M, Woo J-Y, Jee B-C, Hwang Y-K, Yun C-h, Moon S-B, Chung J-H, Kang A-S. Effect of cross-linking agent and heteropolyacid (HPA) contents on physicochemical characteristics of covalently cross-linked sulfonated poly(ether ether ketone)/HPAs composite membranes for water electrolysis. J Ind Eng Chem 2011;17:657−66.

[44] Park JS, Choi HJ, Han GD, Koo J, Kang EH, Kim DH, Bae K, Shim JH. High−performance protonic ceramic fuel cells with a PrBa0.5Sr0.5Co1.5Fe0.5O5+δ cathode with palladium−rich interface coating. J Power Sources 2021;482:229043.

[45] Zhang J, Chen S, Bai H, Lu S, Xiang Y, Jiang SP. Effects of phosphotungstic acid on performance of phosphoric acid doped polyethersulfone-polyvinylpyrrolidone membranes for high temperature fuel cells. Int J Hydrogen Energy 2021;46:11104−14.

[46] Kim K-H, Lee K-Y, Lee S-Y, Cho E, Lim T-H, Kim H-J, Yoon SP, Kim SH, Lim TW, Jang JH. The effects of relative humidity on the performances of PEMFC MEAs with various Nafion® ionomer contents. Int J Hydrogen Energy 2010;35:13104−10.

[47] Zhang J, Tang Y, Song C, Xia Z, Li H, Wang H, Zhang J. PEM fuel cell relative humidity (RH) and its effect on performance at high temperatures. Electrochim Acta 2008;53:5315−21.

[48] Ouattara-Brigaudet M, Berthon-Fabry S, Beauger C, Achard P. Correlations between the catalytic layer composition, the relative humidity and the performance for PEMFC carbon aerogel based membrane electrode assemblies. Int J Hydrogen Energy 2014;39:1420−9.

[49] da Trindade LG, Zanchet L, Martins PC, Borba KMN, Santos RDM, Paiva RdS, Vermeersch LAF, Ticianelli EA, de Souza MO, Martini EMA. The influence of ionic liquids cation on the properties of sulfonated poly (ether ether ketone)/polybenzimidazole blends applied in PEMFC. Polymer 2019;179:121723.